Journal of Clinical & Experimental Ophthalmology

Hunter et al., J Clin Exp Ophthalmol 2014, 5:1
DOI: 10.4172/2155-9570.1000327

Review Article Open Access

Drusen Imaging: A Review

Allan A. Hunter[1,#], **Eric K. Chin**[2,#,*], **David R.P. Almeida**[2] **and David G. Telander**[3]

[1]*Vision Center, Fresno, CA, USA*

[2]*University of Iowa, Department of Ophthalmology & Visual Sciences, Iowa City, IA, USA*

[3]*Sacramento Retinal Consultants, Sacramento, CA, USA*

[#]*Authors made equal contribution to the publication*

[*]**Corresponding author:** Eric K. Chin, M.D., University of Iowa, Department of Ophthalmology and Visual Sciences, 200 Hawkins Dr., Iowa City, IA 52242, USA, Tel: (319) 356-2864; Fax: (319) 356-0363; E-mail: chin.eric@gmail.com

Received date: Dec 30, 2013, **Accepted date:** Feb 19, 2014, **Published date:** Feb 26, 2014

Abstract

Drusen represent the hallmark of non-exudative age-related macular degeneration (AMD). Drusen vary in their location within the retina, ranging from sub-retinal pigment epithelium (RPE) drusen and sub-neurosensory retinal drusenoid deposits above the RPE (or pseudo-drusen). In this paper, we review the rapidly advancing imaging techniques currently available to better correlate drusen volume to clinical stage. This includes, but is not limited to, fundus photography, fluorescein angiography, optical coherence tomography, infrared imaging, fundus autofluorescence, confocal adaptive-optics imaging, and hyperspectral retinal imaging. A new understanding of drusen role in the pathogenesis of the disease may be possible with these imaging modalities in future clinical studies.

Keywords: Age-related macular degeneration; Drusen; Imaging; Color fundus photography; Fluorescein angiography; Optical coherence tomography; Infrared; Autofluorescence; Adaptive optics; Scanning laser ophthalmoscopy; Hyperspectral retinal imaging

Introduction

Age-related macular degeneration (AMD) is the major cause of visual loss in people over the age of 50 years in developed countries [1,2]. The most common form of AMD is the non-exudative variant that represents 90-95% of all AMD cases [3]. The presence of macular large (greater than 125 μm) drusen is a characteristic finding of non-exudative disease and is a key risk factor for the development of more advanced stages [4]. Drusen are historically described as focal deposits of extracellular material located between the basal lamina of the retinal pigment epithelium (RPE) and the inner collagenous layer of Bruch membrane, although sub-retinal drusenoid deposits (SDD) have also been described [5-7]. The latter are more commonly referred to as "pseudodrusen" or "reticular pseudodrusen" and represent a distinct entity; however, both are significantly associated with late AMD [8].

The exact pathogenesis of drusen formation is largely unknown, but given its composition of cellular byproducts from RPE metabolism, and primary location along the basal aspect of these cells, prevailing theories point to an age-associated disruption of cellular machinery in the photoreceptor-RPE complex. Multiple genetic and environmental factors contribute to both the onset and progression of the disease. Numerous longitudinal studies have demonstrated positive correlations between estimated total drusen area and maximum drusen size with risk of progression to advanced AMD using fundus photography [9,10]. Attempts to reduce drusen disease-burden by laser photocoagulation has failed to show visual benefit, to date [11,12].

From clinical observations, drusen are dynamic in size and distribution in the posterior pole, which highlights a potentially active process in their development and maintenance [13]. The requirement for drusen in the clinical diagnosis of AMD and risk-stratification for progression (e.g. soft vs. hard, confluent vs. isolated, bilateral vs. unilateral, small vs. intermediate vs. large), highlights the importance of understanding how drusen appear in ophthalmic imaging. With slit lamp biomicroscopy of the fundus, drusen appear as yellow-white deposits deep to the retina [14], and these changes are often difficult to quantify or qualify for clinical and research purposes. Existing AMD grading systems often require human grader's subjective manual input, which is time consuming and difficult to maintain intra or inter-rater agreement [15]. Due to the high degree of graders' involvement, the methods are prone to inaccuracy and poor repeatability if experienced graders are not used [16]. High-resolution retinal imaging systems have therefore become prominent and powerful diagnostic tools in the field of ophthalmology. It remains unproven the clinical impact of drusen volume determination, but certainly with improved drusen imaging we may better understand the role of drusen in the pathogenesis of the disease.

Color Fundus Photography

Color fundus photographs have been the gold standard to assess the clinical stage of non-exudative AMD and studying the epidemiology of the disease (Figure 1) [15,17]. Among them, the Wisconsin Age-related Maculopathy Grading System, the International Classification and the Grading System for Age-related Maculopathy and Age-related Macular Degeneration and its modified version are widely used [1,15,18].

Figure 1: Color fundus photo of high-risk non-exudative age-related macular degeneration. There are numerous large (greater than 125 micrometer) soft drusen with central confluence in the fovea. Additionally, areas of RPE pigmentation abnormalities can be noted in the areas outside the drusen confluence.

While color photos can provide an en face two-dimensional view of the retina, they can be challenging to reliably quantify and localize drusen against the varying background of macula, RPE, and choroidal pigment [15,19,20]. A qualitative approach to drusen evaluation is likely to be less sensitive to small changes and prone to errors of inter-observer variability. Such an evaluation may also miss early changes of AMD when drusen are often smaller and isolated. Other limitations include inter-patient variability in fundus pigmentation, drusen morphology and indistinct borders, media opacity, and image quality [21]. In a prospective pilot study of eyes with intermediate AMD, Jain et al. described how hyper-pigmentation in color photographs corresponded to intraretinal pigmentary migration on spectral-domain optical coherence tomography with obscuration of underlying large drusen that were not visible on color photographs [22].

Quantification of drusen size and total area covered by drusen is an important risk factor for progression. It has been proposed to use automated software and color fundus imaging with good sensitivity and specificity for detecting drusen and quantifying drusen size and area in the macular region with standard color retinal images [23]. These (semi-) automatic image analysis methods include enhancement and segmentation of drusen. Contrast alteration has been used to improve detail registration prior to software processing. Improved contrast has been investigated with edge detection, clustering-based segmentation techniques, texture edge, and intensity thresholding.

Drusen edge detection uses delta changes in absolute pixel intensity. Soft drusen detection is hindered by their 'feathered', indistinct edges [24]. Clustering-based drusen segmentation aggregates 'similar' image components in clusters [25,26]. Texture-based drusen segmentation uses wavelet analysis to highlight surface contour in multiple orientations [27]. Different image components are separated and analyzed for signal intensity alterations and a 'texture' map is generated from the distribution data [28]. Thresholding-based drusen segmentation uses binary image data of frequency and pixel intensity against a normative background histogram [29]. While the above automated color photographs drusen algorithms are extremely encouraging, soft drusen detection remains problematic due to the difficulty in accurately delineating the blurred margins of large drusen.

A unified, universally accepted AMD classification scheme is lacking. AMD grading systems and severity scales have been developed which are commonly based on standardized grading of color fundus photographs. At present, there is no universally-accepted precise definition of the AMD phenotype for clinical or research purposes [30]. Many classifications incorporate drusen size, character, location, number, area, and level of pigmentation. However, serial studies have shown that drusen are changing frequently in human fundi, whether they be arising de-novo and regressing [31-33]. While late changes in AMD are generally more widely agreed upon, it is the earliest stages of AMD that remain difficult to detect and classify, either by standardized grading systems with highly trained 'readers' or (semi-) automated algorithms of fundus photography [30]. Either way, classifications based on color photographs alone ignore important changes such as the accumulation of autofluorescent material (lipofuscin) in the RPE, the development of reticular pseudodrusen, or the loss of rod photoreceptors [30]. Groups have shown that "pseudo-drusen" in the sub-retinal space appear remarkably similar in fundus photography to sub-RPE drusen [34]. Subretinal drusenoid deposits (SDD) are polymorphous light-grey interconnected accumulations above the RPE. Both cuticular and soft drusen appear yellow due to the removal of shorter wavelength light by a double pass through the RPE whereas SDD (which are located above the RPE) are not subjected to short wavelength attenuation and therefore are more prominent when viewed with blue light [35]. Therefore, the presence of small satellites of atrophy and the impossibility to detect three-dimensional anatomic information of retinal abnormalities limits the use of color photographs alone in drusen detection [36].

Fluorescein Angiography

Our understanding of drusen composition and distribution in the retina is greatly enhanced by each new funduscopic imaging modality's ability to characterize these heterogeneous, extracellular, predominately-lipoprotein aggregates [37-39]. Hard and soft drusen, cuticular drusen and reticular pseudodrusen have different imaging characteristics. Fluorescein angiography's (FA) ability to combine red-free fundus photography and autofluorescence with additional dynamic information on the choroidal and retinal vasculature status (e.g., fluorescein staining of drusen or drusenoid pigment epithelial detachments, and "starry-sky" fundus) has aided understanding of the disease [40-41].

Soft drusen in autofluorescence imaging show hyper-autofluorescence of the borders compared to the center, which is more apparent with camera-based images than with scanning laser ophthalmoscope (SLO) images [42]. During FA, soft drusen can exhibit variable, late hyperfluorescence. Cuticular drusen are smaller in diameter, normally 50-75 microns, and are easily recognized in FA by their tight funduscopic grouping as circular punctate yellow lesions that exhibit central hypo-autofluorescence and central hyper-fluorescence in FA (Figure 2). This has been shown to be due to the RPE attenuation at the apices of cuticular drusen, a unique finding in comparison to hard drusen and reticular pseudodrusen [43,44]. The diminished concentration of cytosolic RPE melanin and lipofuscin at the center of cuticular drusen allow for greater fluorescence

transmission and a decreased autofluorescence signal. Reticular pseudo-drusen is harder to identify with FA showing no change to minimal hypofluorescence [45].

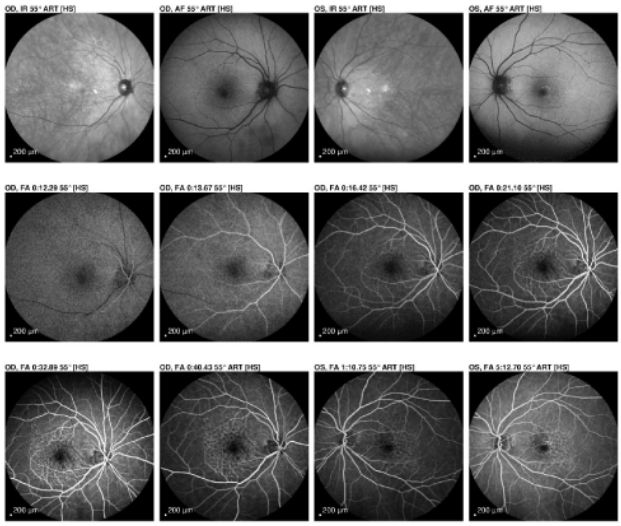

Figure 2: Cuticular drusen.
IR: Red Free; AF: Autofluorescence; FA: Fluorescein Angiography
The cuticular drusen detailed are somewhat lost in the IR images, but highlighted by the hypo-autofluorescent centers in AF images and hyper-fluorescent centers in FA images.

Optical Coherence Tomography

Spectral-domain optical coherence tomography (SD-OCT) is a non-invasive, high-resolution imaging modality capable of producing high-speed three-dimensional cross-sectional images covering the central macula (Figure 3). It provides both qualitative information, such as ultrastructural changes during follow-up [46], and quantitative parameters, such as area and volume of the studied lesions. It also allows for cross-sectional visualization that characterizes microstructural alterations in the different laminae of the retina [47]. While OCT is a useful tool for the visualization of drusen, an objective assessment of drusen is limited by the lack of a method to robustly quantify these lesions on serial OCT images. Macular volume scans are also non-continuous over the macula area depending on which scanning protocol is used (e.g. five line raster versus radial scans). With automated fundus registration, serial scans illuminate the same portion of the macula with good reproducibility and improved assessment of pathology over time. Despite software advancements and image registration, a large portion of the macula is never visualized. Serial macula scan's 'reproducibility' on some OCT machines can create a limited effective clinical-map 'volume'.

It has already been shown by numerous articles that drusen position and composition change with time [31-33]. If a large portion of the macula is skipped with automated registration, drusen volume determination is at best an estimation. Automatic drusen segmentation methods have been proposed to help solve this problem. The RPE and Bruch's membrane can be automatically delineated in SD-OCT images allowing quantification of the elevated RPE segment [48,49].

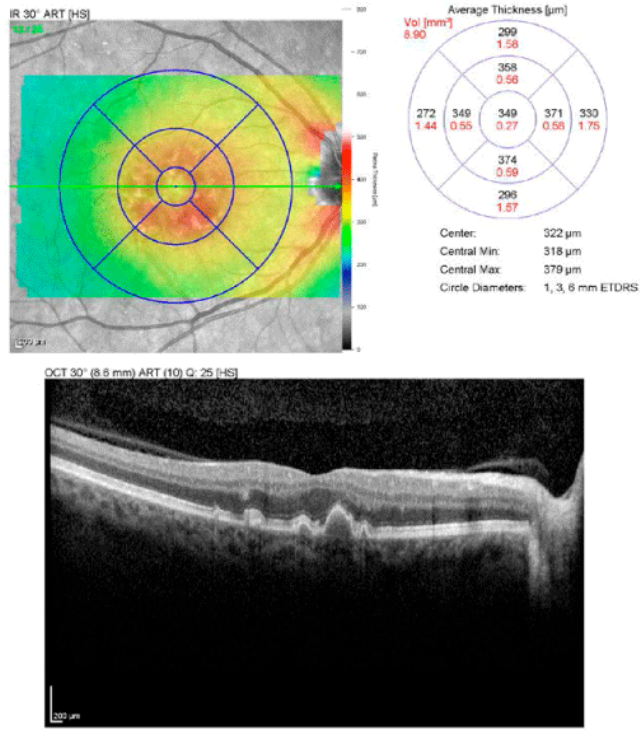

Figure 3: Optical coherence tomography (OCT) imaging of non-exudative age-related macular degeneration exemplifying automated output measures such as macular volume and central macular thickness measurements. While OCT imaging with automated fundus registration allows for serial reproducible imaging of the same area of the macula, there is no accessible algorithm that tracks drusen changes over time.

This technology must be coupled with an improved OCT-determined effective drusen volume (EDV) that more accurately reflects the actual drusen burden. While limiting inter-scan distances to drusen borders may be helpful, performing additional raster scans of the macula is time-consuming and may degrade image quality and accuracy. Eye tracking may counteract this to increase the quality scans [50,51]. The Spectralis HRA2, for example, allows for foveal centration during the longer exam times.

OCT scanning density has been studied in SD-OCT for choroidal volume measurements and an inter-scan distance of 480 µm was determined 'clinically relevant and reliable' [52]. Macula volume OCT reproducibility has been studied between time-domain OCT and newer SD-OCT [53]. When faster OCT (SD-OCT) technologies with greater radial scan density were used, errors of measurements were reduced. If reliable drusen thickness and volume measurements were possible with fewer scans, the time required for the raster scans and the effect of eye movements could be reduced. No study to date has determined the impact of reducing the B-scan density on drusen volume determination.

Measurement of drusen on SD-OCT may become an important imaging biomarker to enable sensitive assessment for change in disease status, response to treatment, or progression. Individual drusen are not routinely measured on SD-OCT because doing this manually is time-consuming. In addition, there are different types of

drusen, some more or less amenable to automated segmentation. Khanifar et al categorized drusen ultrastructure using SD-OCT according to four morphologic parameters: shape, predominant internal reflectivity, homogeneity, and presence of overlying hyper-reflective foci [54].

Reticular pseudodrusen are found in the fundus of some patients with AMD (Figure 4). They are associated with subretinal drusenoid deposits, which are described as material that lies above the RPE [8]. This is in contrast to traditional drusen that are below the RPE, a distinction that wasn't made definitely possible until OCT. Zweifel et al. [8] suggested that the hyper-reflective material could be graded by thickness of the accumulation above the RPE using OCT and proposed a defined grading system of three stages. According to their grading system, stage 1 is characterized by diffuse deposition of granular hyper-reflective material between the RPE and the boundary between the inner and outer segments (IS-OS) of the photoreceptors. In stage 2, mounds of accumulated materials are sufficient to alter the contour of the IS-OS boundary. And lastly, in stage 3, the material is thicker, adopts a conical appearance, and breaks through the IS-OS boundary.

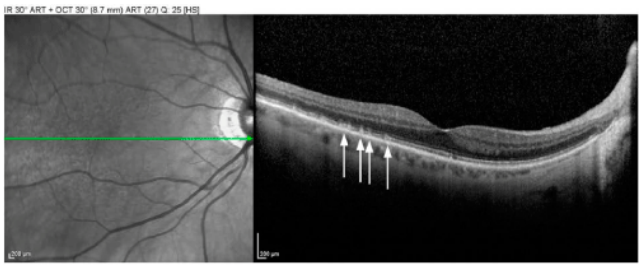

Figure 4: Pseudo-drusen are best distinguished from standard drusen via optical coherence tomography. Whereas cuticular drusen and soft drusen appear as round punctate accumulations under the retinal pigment epithelium (RPE), pseudo-drusen (or subretinal drusenoid deposits) are interconnected accumulations above the RPE.

Good reproducibility has been shown by three-dimensional SD-OCT in non-exudative AMD [55]. Systems combining SD-OCT with a confocal scanning laser ophthalmoscope (cSLO) allow simultaneous recordings of cross-sectional OCT images with various topographic imaging modes. Additionally, real-time eye-tracking technology in SD-OCT systems allows for precise orientation of the scan toward the region of interest, as well as re-scanning of the region at follow-up [56].

Infrared Imaging

The use of infrared imaging could be advantageous for drusen detection (Figure 5). Infrared light has a deeper penetration with minimal scatter due to media opacities (e.g., cataracts, asteroid hyalosis, syneresis) [57]. There are newer capture systems with aperture-modulation to detect scattered light off the fundus, itself [58]. Elevated structures, such as macular drusen, have a characteristic 'moon surface' pattern that makes their edges more visible [59].

Infrared scanning laser ophthalmoscopy appears to have greater sensitivity for drusen detection than conventional color fundus photographs [60,61]. Additional studies are required to determine the clinical impact, but drusen topographic maps are limited by the sensitivity of drusen capture.

Figure 5: Infrared image of large high-risk drusen.

If the aperture is displaced laterally from the confocal light path, a 'pseudo-three-dimensional image' is possible, allowing detection of drusen as raised structures with more clearly defined boundaries. This is believed to improve the contrast and sensitivity for identifying drusen, which may otherwise be difficult to distinguish in the context of a diffusely thickened Bruch membrane [62]. Unfortunately, robust automated segmentation algorithms are needed to use this data for quantitative purposes. As more powerful software becomes available, detailed drusen classification (maps and volumes) may become a possibility to assist clinical studies and assessments.

Fundus Autofluorescence

Fundus autofluorescence (FAF) using a fundus camera or a cSLO has been extensively studied (Figure 6). FAF generated with short-wavelength excitation is dominated by RPE lipofuscin [63], a complex mixture of visual fluorophores [64] that accumulates in the RPE after photoreceptor outer segment phagocytosis. Lipofuscin is a major constituent of drusen and FAF has been investigated to see if sub-clinical drusen were evident by autofluorescence before fundus photography [65-67].

Large soft foveal drusen often correspond to areas of increased FAF; however, the correlation between the distribution of drusen and AF is otherwise weak [68]. Other limitations to the use of FAF are the difficulty of detecting geographic atrophy (GA) and its boundaries in the presence of advanced cataracts. Also, when using the cSLO-based imaging system, it is sometimes difficult to identify the boundaries of GA in close proximity to the center of the macula because of the retinal xanthophylls that absorb the excitation light and block FAF from the underlying RPE [69].

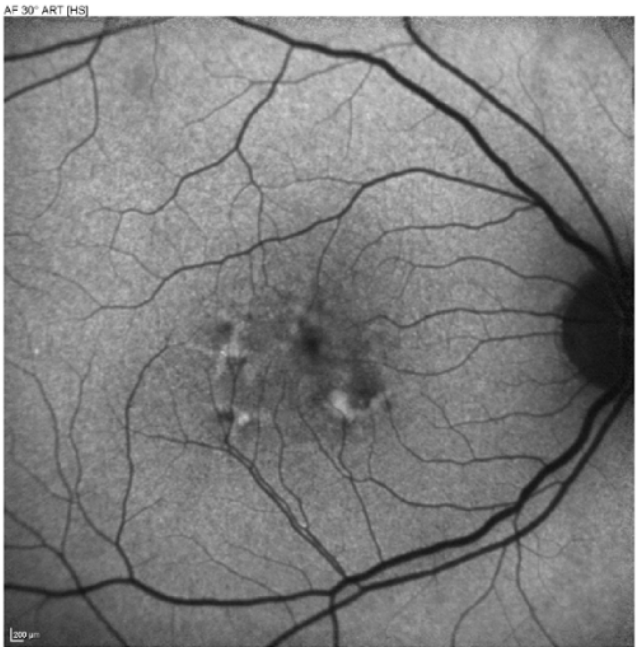

Figure 6: Autofluorescence image of non-exudative age-related macular degeneration. Characteristic changes in autofluorescence imaging at the boundary of drusen can be used to define morphology and determine prognostic significance when assessing various forms of drusen.

Confocal Adaptive Optics Imaging

In vivo imaging can provide high resolution images of the macular photoreceptor mosaic in patients with AMD. However, achieving detailed images of cellular structures within the retina using conventional ophthalmic techniques is limited by optical aberrations produced by ocular tissue, primarily the cornea and lens. Many of these aberrations can be overcome using emerging adaptive optics (AO) retinal imaging techniques to generate an improved imaging of retinal morphology (Figure 7).

AO imaging systems traditionally consist of three principal components which actively measure and correct optical aberrations to achieve heightened resolution. The three primary components of traditional AO systems include: a wavefront sensor, a corrective optical element, and a feedback control system [71]. The wavefront sensor uses a lenslet array and a charged-couple device (CCD) camera to continuously measure distortions in the intensity and shape of the wavefront. The corrective optical element, generally a deformable mirror, compensates for optical aberrations by modifying the shape of the reflective surface. Finally, a software control system is used as an interface between the wavefront sensor and the corrective optical element. These three components work in unison to allow AO imaging systems to correct optical aberrations for enhanced image acquisition.

Since the first demonstration of AO enhanced retinal imaging nearly 15 years ago [72], these techniques have been successfully incorporated into a variety of retinal imaging systems, including fundus camera, SLO [73-75] and OCT [76,77]. Recently, multiple retinal imaging techniques have been combined with AO [70,78]. Adaptive optics-scanning laser ophthalmoscope (AO-SLO) imaging demonstrates slight disruption in the photoreceptor mosaic in early stages of AMD due to focal drusen formation and identified several small drusen deposits that are not observed with standard clinical imaging techniques [79]. Using this technology, an increase in photoreceptor disruption has been visualized within the macula in direct correlation with the stage of AMD progression leading to a decrease in visual acuity [79].

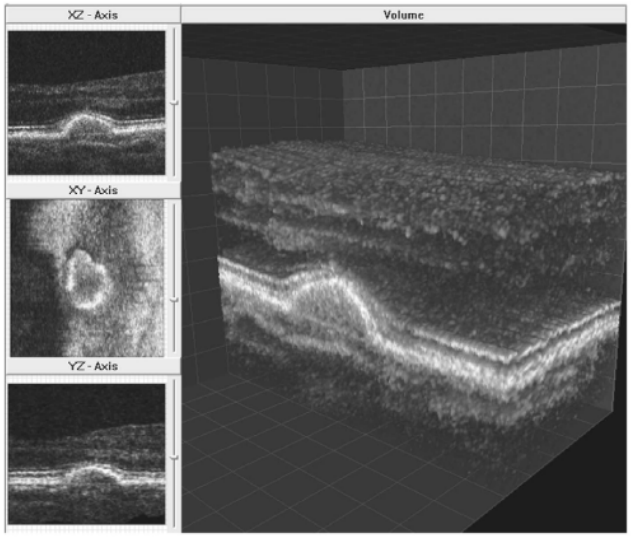

Figure 7: AO-OCT image of a microscopic druse in a patient with age-related macular degeneration. (Reproduced With Permission from Zawadzki RJ et al. [70])

AO retinal imaging systems are currently limited to investigational use but show promise as an enhanced diagnostic imaging technique. Many studies have characterized the distribution of photoreceptors associated with aging and AMD based on histopathology. Recently, AO imaging has been used to assess the variation in cone photoreceptor density in healthy populations based on parameters such as age, eccentricity, eye length, and refractive error [80-83]. By providing cellular resolution of retinal pathology in vivo, AO enhanced imaging may help guide future treatment strategies for numerous retinal diseases such as AMD.

Hyperspectral Retinal Imaging (HRI)

Hyperspectral retinal imaging (HRI) combines different images within the electromagnetic spectrum (EMS) to form an image 'cube' set which encompass a large range of wavelengths. HRI utilizes the visible spectrum and acquires images in three different ways: (1) sequential spatial scanning, (2) stacking of spectral bands, (3) using a "snapshot" by capturing all the spectral and spatial information simultaneously. Spatially or spectrally scanning affords the best resolution at the cost of motion artifact as the data is acquired over time. Recent work has been focused at improving "snapshot" technologies to make use of the lack of motion artifact [84]. By combining multiple wavelengths, HRI has the potential to identify spectral coefficients for macular pigments, drusen subtypes, and (deoxy-) hemoglobin [85-87]. By linking the data to a fundus photograph, the spectral data can have succinct spatial resolution. The

technology has great potential to explore large areas of wavelength in white light which are currently underutilized in ophthalmology. Perhaps composition or positional information of drusen remains to be 'translated' from different spectral coefficient relationships.

Summary

Drusen represent the hallmark of non-exudative AMD and can exist as sub-RPE cuticular or soft drusen and as subretinal drusenoid deposits above the RPE known as pseudo-drusen. With advancing imaging techniques, we may be able to better correlate prognosis and/or response to treatment based on changes in drusen volume. Commercially available fundus photography, fluorescein angiography, infrared imaging, and optical coherence tomography can all aid in monitoring drusen with exceptional level of detail. Perhaps less widely used are autofluorescence, adaptive optics, and hyperspectral imaging; however, these techniques will continue to advance our understanding of the drusen and their role in AMD progression. Rapidly changing software algorithms will also assist in making this process more accurate, reproducible, and perhaps automated.

References

1. Bartlett H, Eperjesi F (2007) Use of fundus imaging in quantification of age-related macular change. Surv Ophthalmol 52: 655-671.
2. Wong TY, Liew G, Mitchell P (2007) Clinical update: new treatments for age-related macular degeneration. Lancet 370: 204-206.
3. Klein R, Chou CF, Klein BE, Zhang X, Meuer SM, et al. (2011) Prevalence of age-related macular degeneration in the US population. Arch Ophthalmol 129: 75-80.
4. Congdon N, O'Colmain B, Klaver CC, Klein R, Muñoz B, et al. (2004) Causes and prevalence of visual impairment among adults in the United States. Arch Ophthalmol 122: 477-485.
5. Sarks SH, Arnold JJ, Killingsworth MC, Sarks JP (1999) Early drusen formation in the normal and aging eye and their relation to age related maculopathy: a clinicopathological study. Br J Ophthalmol 83: 358-368.
6. Abdelsalam A, Del Priore L, Zarbin MA (1999) Drusen in age-related macular degeneration: pathogenesis, natural course, and laser photocoagulation-induced regression. Surv Ophthalmol 44: 1-29.
7. Forte R, Cennamo G, de Crecchio G, Cennamo G (2014) Microperimetry of subretinal drusenoid deposits. Ophthalmic Res 51: 32-36.
8. Zweifel SA, Imamura Y, Spaide TC, Fujiwara T, Spaide RF (2010) Prevalence and significance of subretinal drusenoid deposits (reticular pseudodrusen) in age-related macular degeneration. Ophthalmology 117: 1775-1781.
9. Klein R, Klein BE, Jensen SC, Meuer SM (1997) The five-year incidence and progression of age-related maculopathy: the Beaver Dam Eye Study. Ophthalmology 104: 7-21.
10. Davis MD, Gangnon RE, Lee LY, Hubbard LD, Klein BE, et al. (2005) The Age-Related Eye Disease Study severity scale for age-related macular degeneration: AREDS Report No. 17. Arch Ophthalmol 123: 1484-1498.
11. Complications of Age-related Macular Degeneration Prevention Trial (CAPT) Research Group (2008) Risk factors for choroidal neovascularization and geographic atrophy in the complications of age-related macular degeneration prevention trial. Ophthalmology 115: 1474-1479.
12. Parodi MB, Virgili G, Evans JR (2009) Laser treatment of drusen to prevent progression to advanced age-related macular degeneration. Cochrane Database Syst Rev : CD006537.
13. Complications of Age-Related Macular Degeneration Prevention Trial Research Group (2006) Laser treatment in patients with bilateral large drusen: the complications of age-related macular degeneration prevention trial. Ophthalmology 113: 1974-1986.
14. Schlanitz FG, Ahlers C, Sacu S, Schütze C, Rodriguez M, et al. (2010) Performance of drusen detection by spectral-domain optical coherence tomography. Invest Ophthalmol Vis Sci 51: 6715-6721.
15. Klein R, Davis MD, Magli YL, Segal P, Klein BE, et al. (1991) The Wisconsin age-related maculopathy grading system. Ophthalmology 98: 1128-1134.
16. Niemeijer M, van Ginneken B, Russell SR, Suttorp-Schulten MS, Abràmoff MD (2007) Automated detection and differentiation of drusen, exudates, and cotton-wool spots in digital color fundus photographs for diabetic retinopathy diagnosis. Invest Ophthalmol Vis Sci 48: 2260-2267.
17. Bartlett H, Eperjesi F (2007) Use of fundus imaging in quantification of age-related macular change. Surv Ophthalmol 52: 655-671.
18. Bird AC, Bressler NM, Bressler SB, Chisholm IH, Coscas G, et al. (1995) An international classification and grading system for age-related maculopathy and age-related macular degeneration. The International ARM Epidemiological Study Group. Surv Ophthalmol 39: 367-374.
19. Smith RT, Chan JK, Nagasaki T, Sparrow JR, Barbazetto I (2005) A method of drusen measurement based on reconstruction of fundus background reflectance. Br J Ophthalmol 89: 87-91.
20. Shin DS, Javornik NB, Berger JW (1999) Computer-assisted, interactive fundus image processing for macular drusen quantitation. Ophthalmology 106: 1119-1125.
21. Scholl HP, Peto T, Dandekar S, Bunce C, Xing W, et al. (2003) Inter- and intra-observer variability in grading lesions of age-related maculopathy and macular degeneration. Graefes Arch Clin Exp Ophthalmol 241: 39-47.
22. Jain N, Farsiu S, Khanifar AA, Bearelly S, Smith RT, et al. (2010) Quantitative comparison of drusen segmented on SD-OCT versus drusen delineated on color fundus photographs. Invest Ophthalmol Vis Sci 51: 4875-4883.
23. Bhuiyan A, Karmakar C, Xiao D, Ramamohanarao K, Kanagasingam Y (2013) Drusen quantification for early identification of age related macular degeneration (AMD) using color fundus imaging. Conf Proc IEEE Eng Med Biol Soc 2013: 7392-7395.
24. Parvathi SS, Devi N (2007) Automatic drusen detection from colour retinal images. International Conference on Conference on Computational Intelligence and Multimedia Applications. INSPEC, Tamil Nadu, India.
25. Quellec G, Russell SR, Abramoff MD (2011) Optimal filter framework for automated, instantaneous detection of lesions in retinal images. IEEE Trans Med Imaging 30: 523-533.
26. Hanafi M, Hijazi A, Coenen F, Zheng Y (2010) Retinal image classification for the screening of age-related macular degeneration. SGAI International Conference on Artificial Intelligence AI-2010: 325e338.
27. Brandon L, Hoover A (2003) Drusen detection in a retinal image using multi-level analysis. Medical Image Computing and Computer-Assisted Intervention 2878: 618-625.
28. Kose C, Sevik U, GenÃ§alioÄŸlu O, IkibaÅŸ C, KayikiÃ§ioÄŸlu T (2010) A statistical segmentation method for measuring age-related macular degeneration in retinal fundus images. J Med Syst 34: 1-13.
29. Soliz P, Wilson M, Nemeth S, Nguyen P (2002) Computer-aided methods for quantitative assessment of longitudinal changes in retinal images presenting with maculopathy. SPIE Proceedings of Medical Imaging: Visualization, Image-guided Procedures and Display. 4681: 159-170.
30. Ferris FL 3rd, Wilkinson CP, Bird A, Chakravarthy U, Chew E, et al. (2013) Clinical classification of age-related macular degeneration. Ophthalmology 120: 844-851.
31. Smith RT, Sohrab MA, Pumariega N, Chen Y, Chen J, et al. (2010) Dynamic soft drusen remodelling in age-related macular degeneration. Br J Ophthalmol 94: 1618-1623.
32. Querques G, Kamami-Levy C, Georges A, Pedinielli A, Souied EH (2014) Appearance of regressing drusen on adaptive optics in age-related macular degeneration. Ophthalmology 121: 611-612.

33. Querques G, Georges A2, Ben Moussa N2, Sterkers M2, Souied EH2 (2014) Appearance of regressing drusen on optical coherence tomography in age-related macular degeneration. Ophthalmology 121: 173-179.
34. Lee MY, Ham DI (2014) Subretinal drusenoid deposits with increased autofluorescence in eyes with reticular pseudodrusen. Retina 34: 69-76.
35. Spaide RF, Curcio CA (2010) Drusen characterization with multimodal imaging. Retina 30: 1441-1454.
36. Pirbhai A, Sheidow T, Hooper P (2005) Prospective evaluation of digital non-stereo color fundus photography as a screening tool in age-related macular degeneration. Am J Ophthalmol 139: 455-461.
37. WOLTER JR, FALLS HF (1962) Bilateral confluent drusen. Arch Ophthalmol 68: 219-226.
38. Pauleikhoff D, Zuels S, Sheraidah GS, Marshall J, Wessing A, et al. (1992) Correlation between biochemical composition and fluorescein binding of deposits in Bruch's membrane. Ophthalmology 99: 1548-1553.
39. Curcio CA, Millican CL, Bailey T, Kruth HS (2001) Accumulation of cholesterol with age in human Bruch's membrane. Invest Ophthalmol Vis Sci 42: 265-274.
40. Gass JD, Jallow S, Davis B (1985) Adult vitelliform macular detachment occurring in patients with basal laminar drusen. Am J Ophthalmol 99: 445-459.
41. Sarks SH, Arnold JJ, Killingsworth MC, Sarks JP (1999) Early drusen formation in the normal and aging eye and their relation to age related maculopathy: a clinicopathological study. Br J Ophthalmol 83: 358-368.
42. Delori FC, Fleckner MR, Goger DG, Weiter JJ, Dorey CK (2000) Autofluorescence distribution associated with drusen in age-related macular degeneration. Invest Ophthalmol Vis Sci 41: 496-504.
43. Sarks JP1, Sarks SH, Killingsworth MC (1994) Evolution of soft drusen in age-related macular degeneration. Eye (Lond) 8 : 269-283.
44. Spaide RF, Curcio CA (2010) Drusen characterization with multimodal imaging. Retina 30: 1441-1454.
45. Prenner JL, Rosenblatt BJ, Tolentino MJ, Ying GS, Javornik NB, et al. (2003) Risk factors for choroidal neovascularization and vision loss in the fellow eye study of CNVPT. Retina 23: 307-314.
46. Helb HM, Charbel Issa P, Fleckenstein M, Schmitz-Valckenberg S, Scholl HP, et al. Clinical evaluation of simultaneous confocal scanning laser ophthalmoscopy imaging combined with high-resolution, spectral-domain optical coherence tomography. Acta Ophthalmol 88: 842-849.
47. Hee MR, Baumal CR, Puliafito CA, Duker JS, Reichel E, et al. (1996) Optical coherence tomography of age-related macular degeneration and choroidal neovascularization. Ophthalmology 103: 1260-1270.
48. Schlanitz FG, Ahlers C, Sacu S, Schütze C, Rodriguez M, et al. (2010) Performance of drusen detection by spectral-domain optical coherence tomography. Invest Ophthalmol Vis Sci 51: 6715-6721.
49. Chen Q, Leng T, Zheng L, Kutzscher L, Ma J, et al. (2013) Automated drusen segmentation and quantification in SD-OCT images. Med Image Anal 17: 1058-1072.
50. Menke MN, Dabov S, Knecht P, Sturm V (2009) Reproducibility of retinal thickness measurements in healthy subjects using spectralis optical coherence tomography. Am J Ophthalmol 147: 467-472.
51. Chin EK, Sedeek RW, Li Y, Beckett L, Redenbo E, et al. (2012) Reproducibility of macular thickness measurement among five OCT instruments: effects of image resolution, image registration, and eye tracking. Ophthalmic Surg Lasers Imaging 43: 97-108.
52. Chhablani J, Barteselli G, Bartsch DU, Kozak I, Wang H, et al. (2013) Influence of scanning density on macular choroidal volume measurement using spectral-domain optical coherence tomography. Graefes Arch Clin Exp Ophthalmol 251: 1303-1309.
53. Huang J, Liu X, Wu Z, Xiao H, Dustin L, et al. (2009) Macular thickness measurements in normal eyes with time-domain and Fourier-domain optical coherence tomography. Retina 29: 980-987.
54. Khanifar AA, Koreishi AF, Izatt JA, Toth CA (2008) Drusen ultrastructure imaging with spectral domain optical coherence tomography in age-related macular degeneration. Ophthalmology 115: 1883-1890.
55. Menke MN, Dabov S, Knecht P, Sturm V (2011) Reproducibility of retinal thickness measurements in patients with age-related macular degeneration using 3D Fourier-domain optical coherence tomography (OCT) (Topcon 3D-OCT 1000). Acta Ophthalmol 89: 346-351.
56. Querques G, Canouï-Poitrine F, Coscas F, Massamba N, Querques L, et al. (2012) Analysis of progression of reticular pseudodrusen by spectral domain-optical coherence tomography. Invest Ophthalmol Vis Sci 53: 1264-1270.
57. Elsner AE, Burns SA, Weiter JJ, Delori FC (1996) Infrared imaging of sub-retinal structures in the human ocular fundus. Vision Res 36: 191-205.
58. Manivannan A, Kirkpatrick JN, Sharp PF, Forrester JV (1994) Clinical investigation of an infrared digital scanning laser ophthalmoscope. Br J Ophthalmol 78: 84-90.
59. Diniz B, Ribeiro RM, Rodger DC, Maia M, Sadda S (2013) Drusen detection by confocal aperture-modulated infrared scanning laser ophthalmoscopy. Br J Ophthalmol 97: 285-290.
60. Acton JH, Cubbidge RP, King H, Galsworthy P, Gibson JM (2011) Drusen detection in retro-mode imaging by a scanning laser ophthalmoscope. Acta Ophthalmol 89: e404-411.
61. Ishiko S, Akiba J, Horikawa Y, Yoshida A (2002) Detection of drusen in the fellow eye of Japanese patients with age-related macular degeneration using scanning laser ophthalmoscopy. Ophthalmology 109: 2165-2169.
62. Diniz B, Ribeiro R, Heussen FM, Maia M, Sadda S (2014) Drusen measurements comparison by fundus photograph manual delineation versus optical coherence tomography retinal pigment epithelial segmentation automated analysis. Retina 34: 55-62.
63. Delori FC, Dorey CK, Staurenghi G, Arend O, Goger DG, et al. (1995) In vivo fluorescence of the ocular fundus exhibits retinal pigment epithelium lipofuscin characteristics. Invest Ophthalmol Vis Sci 36: 718-729.
64. Sparrow JR, Fishkin N, Zhou J, Cai B, Jang YP, et al. (2003) A2E, a byproduct of the visual cycle. Vision Res 43: 2983-2990.
65. Landa G, Rosen RB, Pilavas J, Garcia PM (2012) Drusen characteristics revealed by spectral-domain optical coherence tomography and their corresponding fundus autofluorescence appearance in dry age-related macular degeneration. Ophthalmic Res 47: 81-86.
66. Delori FC1, Fleckner MR, Goger DG, Weiter JJ, Dorey CK (2000) Autofluorescence distribution associated with drusen in age-related macular degeneration. Invest Ophthalmol Vis Sci 41: 496-504.
67. Fujimura S1, Ueta T, Takahashi H, Obata R, Smith RT, et al. (2013) Characteristics of fundus autofluorescence and drusen in the fellow eyes of Japanese patients with exudative age-related macular degeneration. Graefes Arch Clin Exp Ophthalmol 251: 1-9.
68. Lois N, Owens SL, Coco R, Hopkins J, Fitzke FW, et al. (2002) Fundus autofluorescence in patients with age-related macular degeneration and high risk of visual loss. Am J Ophthalmol 133: 341-349.
69. Schmitz-Valckenberg S, Fleckenstein M, Göbel AP, Sehmi K, Fitzke FW, et al. (2008) Evaluation of autofluorescence imaging with the scanning laser ophthalmoscope and the fundus camera in age-related geographic atrophy. Am J Ophthalmol 146: 183-192.
70. Zawadzki RJ, Choi SS, Jones SM, Oliver SS, Werner JS (2007) Adaptive optics-optical coherence tomography: optimizing visualization of microscopic retinal structures in three dimensions. J Opt Soc Am A Opt Image Sci Vis 24: 1373-1383.
71. Porter J (2006) Adaptive optics for vision science: Principles, practices, design, and applications. Wiley-Interscience, Hoboken, NJ.
72. Liang J, Williams DR, Miller DT (1997) Supernormal vision and high-resolution retinal imaging through adaptive optics. J Opt Soc Am A Opt Image Sci Vis 14: 2884-2892.
73. Roorda A, Romero-Borja F, Donnelly Iii W, Queener H, Hebert T, et al. (2002) Adaptive optics scanning laser ophthalmoscopy. Opt Express 10: 405-412.

74. Zhang Y, Poonja S, Roorda A (2006) MEMS-based adaptive optics scanning laser ophthalmoscopy. Opt Lett 31: 1268-1270.

75. Burns SA, Tumbar R, Elsner AE, Ferguson D, Hammer DX (2007) Large-field-of-view, modular, stabilized, adaptive-optics-based scanning laser ophthalmoscope. J Opt Soc Am A Opt Image Sci Vis 24: 1313-1326.

76. Miller DT, Kocaoglu OP, Wang Q, Lee S (2011) Adaptive optics and the eye (super resolution OCT). Eye (Lond) 25: 321-330.

77. Zhang Y, Cense B, Rha J, Jonnal RS, Gao W, et al. (2006) High-speed volumetric imaging of cone photoreceptors with adaptive optics spectral-domain optical coherence tomography. Opt Express 14: 4380-4394.

78. Mujat M, Ferguson RD, Patel AH, Iftimia N, Lue N, et al. (2010) High resolution multimodal clinical ophthalmic imaging system. Opt Express 18: 11607-11621.

79. Boretsky A, Khan F, Burnett G, Hammer DX, Ferguson RD, et al. (2012) In vivo imaging of photoreceptor disruption associated with age-related macular degeneration: A pilot study. Lasers Surg Med 44: 603-610.

80. Song H, Chui TY, Zhong Z, Elsner AE, Burns SA (2011) Variation of cone photoreceptor packing density with retinal eccentricity and age. Invest Ophthalmol Vis Sci 52: 7376-7384.

81. Chui TY, Song H, Burns SA (2008) Adaptive-optics imaging of human cone photoreceptor distribution. J Opt Soc Am A Opt Image Sci Vis 25: 3021-3029.

82. Li KY, Tiruveedhula P, Roorda A (2010) Intersubject variability of foveal cone photoreceptor density in relation to eye length. Invest Ophthalmol Vis Sci 51: 6858-6867.

83. Chui TY, Song H, Burns SA (2008) Individual variations in human cone photoreceptor packing density: variations with refractive error. Invest Ophthalmol Vis Sci 49: 4679-4687.

84. Johnson WR, Wilson DW, Bearman G (2006) Spatial-spectral modulating snapshot hyperspectral imager. Appl Opt 45: 1898-1908.

85. Lee N, Wielaard J, Fawzi AA, Sajda P, Laine AF, et al. (2010) In vivo snapshot hyperspectral image analysis of age-related macular degeneration. Conf Proc IEEE Eng Med Biol Soc 2010: 5363-5366.

86. Johnson WR, Wilson DW, Fink W, Humayun M, Bearman G (2007) Snapshot hyperspectral imaging in ophthalmology. J Biomed Opt 12: 014036.

87. Mordant DJ, Al-Abboud I, Muyo G, Gorman A, Sallam A, et al. (2011) Spectral imaging of the retina. Eye (Lond) 25: 309-320.

This article was originally published in a special issue, entitled: **"Age Related Macular Degeneration",** Edited by Dr. Stephen G Schwartz, Bascom Palmer Eye Institute at Naples, USA and Prof. Ayman Ahmed Alkawas, Zagazig University, Egypt